

Supporting Information

Study of the antimalarial activity of 4-aminoquinoline compounds against chloroquine sensitive and chloroquine resistant parasite strains

Alexandre S. Lawrenson, David L. Cooper, Paul M. O'Neill, Neil G. Berry*

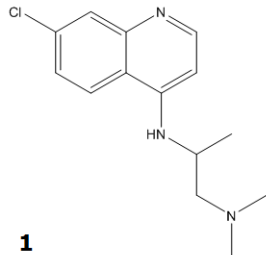
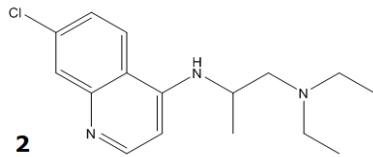
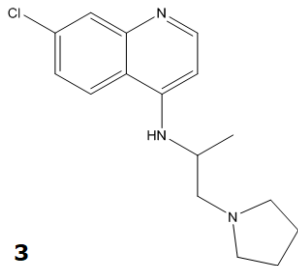
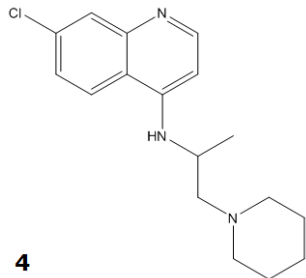
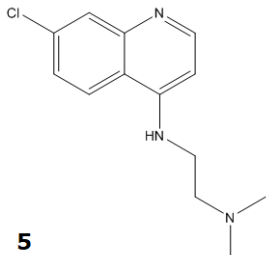
Department of Chemistry, University of Liverpool, Liverpool L69 7ZD, UK

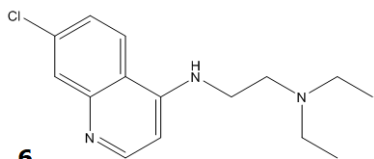
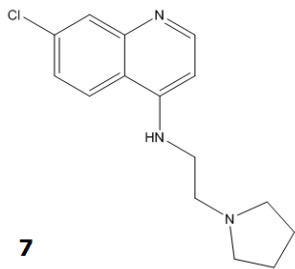
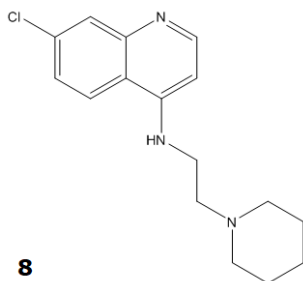
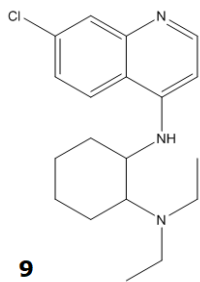
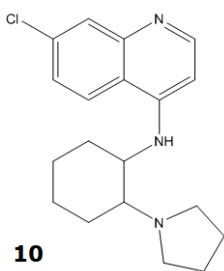
*Corresponding author: ngberry@liverpool.ac.uk

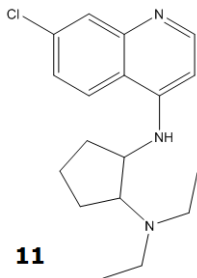
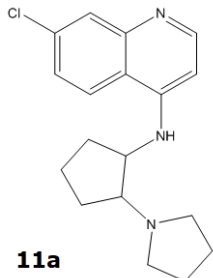
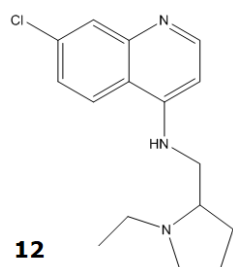
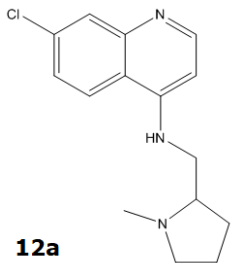
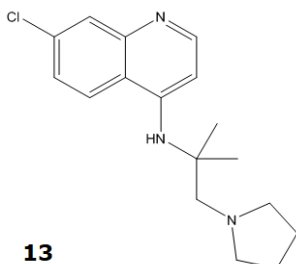
Contents

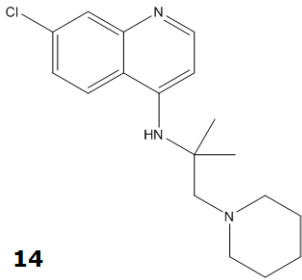
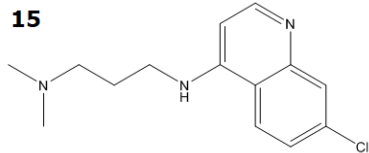
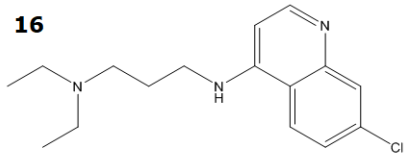
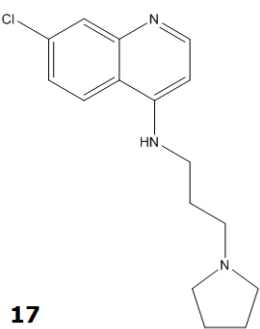
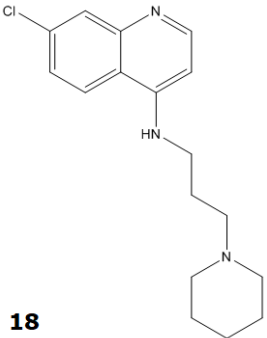
Chemical structures and IC ₅₀ values	2
Partial least squares models for NF54 and K1 pIC ₅₀ values	11

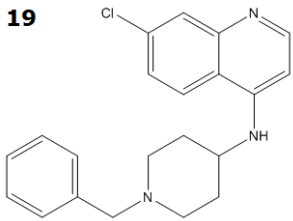
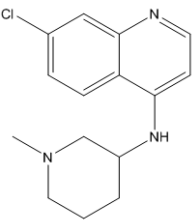
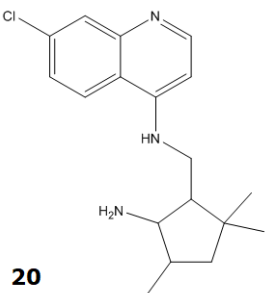
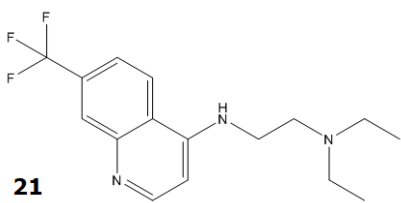
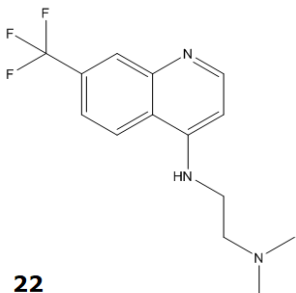
Table S1 The 4-aminoquinoline structures together with their IC₅₀ values for the NF54 and K1 strains. RMM denotes the relative molecular mass used in the conversion to pIC₅₀ values (see main text).

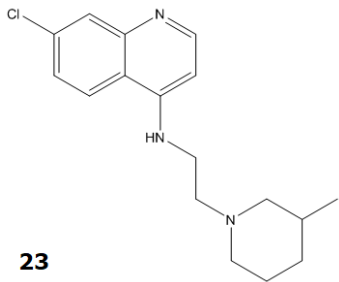
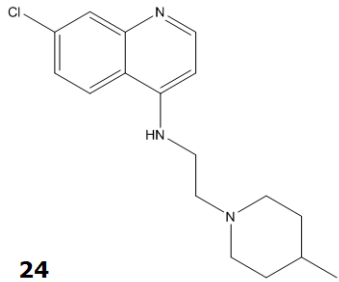
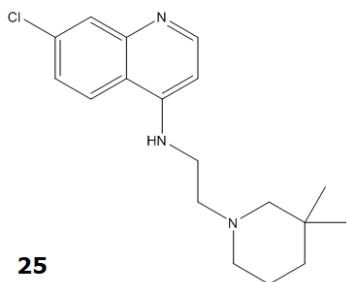
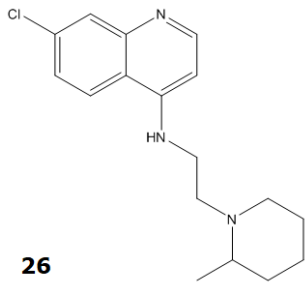
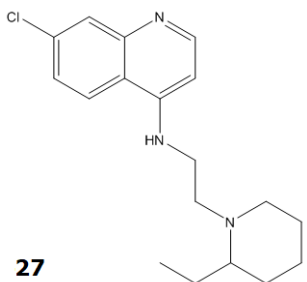
Compound	IC ₅₀ (ng/ml)		RMM
	NF54	K1	
<p>1</p> 	4	9	263.77
<p>2</p> 	7	14	291.82
<p>3</p> 	7	12	289.8
<p>4</p> 	7	15	303.83
<p>5</p> 	4	7	249.74

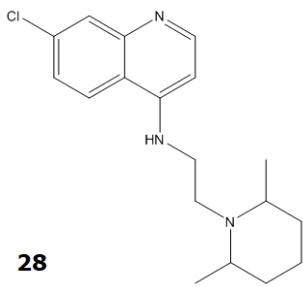
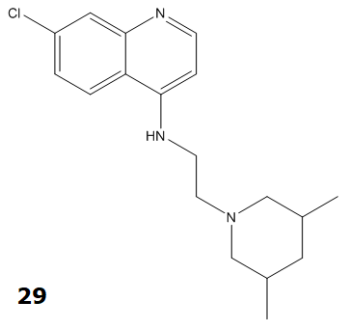
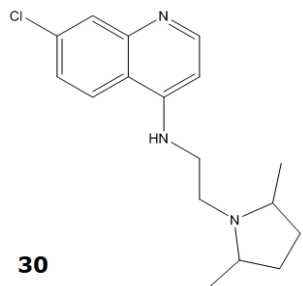
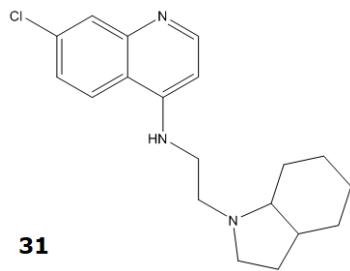
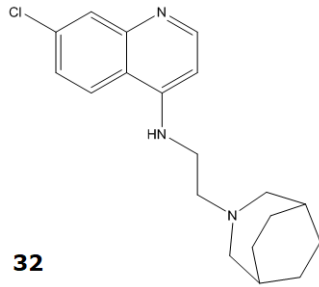
Compound	IC ₅₀ (ng/ml)		RMM
	NF54	K1	
6 	4	9	277.79
7 	4	8	275.78
8 	5	11	289.8
9 	11	32	331.88
10 	7	17	329.87

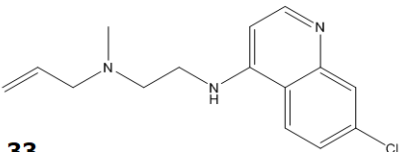
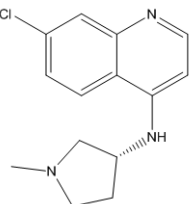
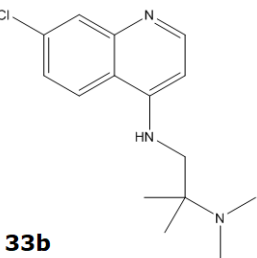
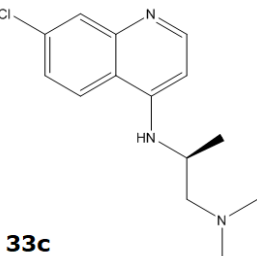
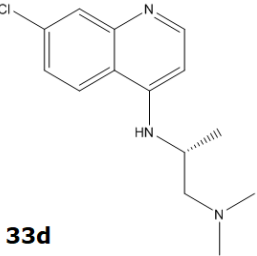
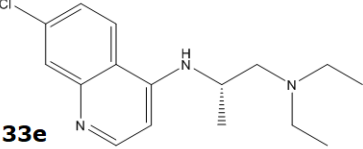
Compound	IC ₅₀ (ng/ml)		RMM
	NF54	K1	
 11	5	18	317.86
 11a	7	15	315.84
 12	6	10	289.8
 12a	7	9	275.78
 13	30	47	303.83

Compound	IC ₅₀ (ng/ml)		RMM
	NF54	K1	
<p>14</p> 	9	21	317.86
<p>15</p> 	2	6	263.77
<p>16</p> 	3	9	291.82
<p>17</p> 	3	15	289.8
<p>18</p> 	4	14	303.83

Compound	IC ₅₀ (ng/ml)		RMM
	NF54	K1	
19 	7	9	351.87
 19a	6	9	275.78
 20	3	10	317.86
 21	21	34	311.35
 22	14	22	283.29

Compound	IC ₅₀ (ng/ml)		RMM
	NF54	K1	
<div>  <p>23</p> </div>	6	15	303.83
<div>  <p>24</p> </div>	7	15	303.83
<div>  <p>25</p> </div>	8	22	317.86
<div>  <p>26</p> </div>	7	15	303.83
<div>  <p>27</p> </div>	8	18	317.86

Compound	IC ₅₀ (ng/ml)		RMM
	NF54	K1	
28 	7	16	317.86
29 	6	16	317.86
30 	7	14	303.83
31 	5	11	329.87
32 	7	16	329.87

Compound	IC ₅₀ (ng/ml)		RMM
	NF54	K1	
 33	8	14	275.78
 33a	7	8	261.75
 33b	8	17	277.79
 33c	8	24	263.77
 33d	8	23	263.77
 33e	12	53	291.82

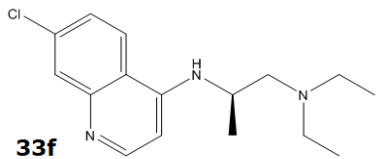
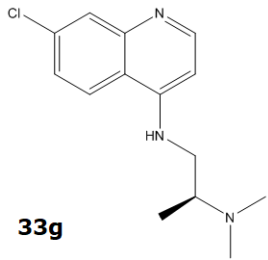
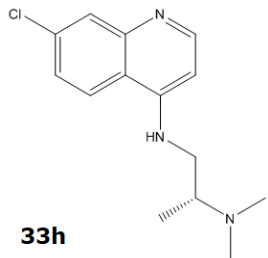
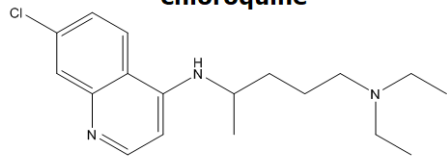
Compound	IC ₅₀ (ng/ml)		RMM
	NF54	K1	
 <p>33f</p>	12	41	291.82
 <p>33g</p>	5	17	263.77
 <p>33h</p>	7	18	263.77
<p>chloroquine</p> 	8	114	319.87

Table S2 Weights (signed) and standard deviations for the most successful of the partial least squares models for NF54 and K1 pIC50 values. Brief explanations of the descriptors are provided. For further information see Todeschini, R. and Consonni, V., Molecular Descriptors for Chemoinformatics (Wiley-VCH, 2009).

NF54 (model 19)		(constant: 7.659615)	
Descriptor	weight (signed)	standard deviation	Brief description
Hy	8.098812×10^{-2}	-8.267599×10^{-2}	Hydrophilic factor
Mor31m	-5.441592×10^{-2}	-5.555000×10^{-2}	3D MoRSE descriptor signal 31 weighted by mass
RDF055m	4.671217×10^{-2}	-4.768570×10^{-2}	Radial Distribution Function weighted by mass
JGI5	-4.627998×10^{-2}	-4.724450×10^{-2}	Mean topological charge index order 5
H-046	4.599253×10^{-2}	-4.695107×10^{-2}	H attached to C0(sp3) no X attached next to C
GATS7p	4.405107×10^{-2}	-4.496914×10^{-2}	Geary autocorrelation of lag 7 weighted by polarizability
Mor31e	-4.339595×10^{-2}	-4.430037×10^{-2}	3D MoRSE descriptor weighted by Sanderson electronegativity
HARD	-3.973951×10^{-2}	-4.056772×10^{-2}	Hardness
GGI1	-3.684569×10^{-2}	-3.761359×10^{-2}	Topological charge index of order 1
DIPX	-3.651527×10^{-2}	-3.727628×10^{-2}	Dipole Moment X
Mor29m	-3.626209×10^{-2}	-3.701782×10^{-2}	3D-MoRSE descriptor signal 29 weighted by mass
H5m	-3.600808×10^{-2}	-3.675852×10^{-2}	GETAWAY descriptor autocorrelation of lag 5 weighted by mass
H5p	-3.436139×10^{-2}	-3.507752×10^{-2}	GETAWAY descriptor autocorrelation of lag 5 weighted by polarisability
HATS8m	-3.040015×10^{-2}	-3.103372×10^{-2}	GETAWAY descriptor autocorrelation of lag 8 weighted by mass
X2Av	2.797397×10^{-2}	-2.855698×10^{-2}	Average valence connectivity index of order 2
E3u	-2.783525×10^{-2}	-2.841537×10^{-2}	3rd component accessibility directional WHIM index
FDI	-2.760407×10^{-2}	-2.817936×10^{-2}	Distance/distance matrix (G/D) leading eigenvalue from distance/distance matrix
DIPY	-2.523651×10^{-2}	-2.576246×10^{-2}	Dipole Moment Y
Mor24e	-2.448182×10^{-2}	-2.499205×10^{-2}	3D-MoRSE descriptor signal 24 weighted by Sanderson electronegativity
Rings count	2.162620×10^{-2}	-2.207691×10^{-2}	Rings count
E2s	2.119065×10^{-2}	-2.163229×10^{-2}	2nd component accessibility directional WHIM index weighted by I-state
H7m	-2.010254×10^{-2}	-2.052150×10^{-2}	GETAWAY descriptor H autocorrelation of lag 7 weighted by mass
PCHGMH	-1.993613×10^{-2}	-2.035162×10^{-2}	Mean partial charge on H atoms
G3p	1.668682×10^{-2}	-1.703459×10^{-2}	3rd component symmetry directional WHIM index weighted by polarizability

GATS4e	-1.566494×10^{-2}	-1.599142×10^{-2}	Geary autocorrelation of lag 4 weighted by Sanderson electronegativity
C-008	-1.511917×10^{-2}	-1.543426×10^{-2}	CHR2X
SCOUNT(C-atom)	1.501300×10^{-2}	-1.532589×10^{-2}	Substructure count
RDF035e	1.326425×10^{-2}	-1.354069×10^{-2}	Radial Distribution Function 035 weighted by Sanderson electronegativity
RDF050m	1.225899×10^{-2}	-1.251448×10^{-2}	Radial Distribution Function 050 weighted by mass
R1e	1.221430×10^{-2}	-1.246886×10^{-2}	GETAWAY descriptor R autocorrelation of lag 1 weighted by Sanderson electronegativity
Mor20e	1.159119×10^{-2}	-1.183277×10^{-2}	3D-MoRSE descriptor signal 20 weighted by Sanderson electronegativity
R3u+	-1.014137×10^{-2}	-1.035272×10^{-2}	GETAWAY descriptor R maximal autocorrelation of lag 3 unweighted
G3u	8.714810×10^{-3}	-8.896436×10^{-3}	WHIM descriptor 3rd component symmetry directional
R4p	-8.605457×10^{-3}	-8.784804×10^{-3}	GETAWAY descriptor R autocorrelation of lag 4 weighted by polarizability
ENEG	6.431618×10^{-3}	-6.565659×10^{-3}	Electronegativity
DIP	5.434864×10^{-3}	-5.548133×10^{-3}	Dipole Moment
HATS7m	4.885984×10^{-4}	-4.987813×10^{-4}	GETAWAY descriptor leverage-weighted autocorrelation of lag 7 weighted by mass
SCOUNT(N-atom)	0	0	Substructure count

Table S2 (continued)

K1 (model 20)			(constant: 7.278025)
Descriptor	weight (signed)	standard deviation	Brief description
Mor31e	-8.279356×10^{-2}	-7.520413×10^{-2}	3D MoRSE descriptor weighted by Sanderson electronegativity
HARD	-8.246118×10^{-2}	-7.490222×10^{-2}	Hardness
Mor31m	-6.313831×10^{-2}	-5.735062×10^{-2}	3D MoRSE descriptor signal 31 weighted by mass
Count of rotatable bond	-5.962762×10^{-2}	-5.416174×10^{-2}	Count of rotatable bond
RDF030m	5.608514×10^{-2}	-5.094399×10^{-2}	Radial Distribution Function 030 weighted by mass
BELp3	5.600810×10^{-2}	-5.087401×10^{-2}	Lowest eigenvalue n. 3 of Burden matrix weighted by atomic polarizabilities
J3D	-5.427589×10^{-2}	-4.930059×10^{-2}	Balaban-like index from geometrical matrix 3D matrix-based descriptors
HATS7p	-4.883058×10^{-2}	-4.435443×10^{-2}	GETAWAY descriptor leverage-weighted autocorrelation of lag 7 weighted by polarisability
R8e	-4.511822×10^{-2}	-4.098237×10^{-2}	GETAWAY descriptor R autocorrelation of lag 8 weighted by Sanderson electronegativity
H5p	-4.391553×10^{-2}	-3.988993×10^{-2}	GETAWAY descriptor H autocorrelation of lag 5 weighted by polarizability
Rings count	4.351619×10^{-2}	-3.952719×10^{-2}	Rings count
DIPY	-3.558066×10^{-2}	-3.231909×10^{-2}	Dipole moment Y
LOGP	-3.392758×10^{-2}	-3.081755×10^{-2}	Moriguchi octanol-water partition coefficient
Mor04e	3.334596×10^{-2}	-3.028924×10^{-2}	3D MoRSE descriptor signal 4 weighted by Sanderson electronegativity
nCt	-3.264431×10^{-2}	-2.965191×10^{-2}	Number of total tertiary C(sp ³)
As	-3.198719×10^{-2}	-2.905502×10^{-2}	WHIM descriptor A total size weighted by I-state
E3u	-3.080757×10^{-2}	-2.798353×10^{-2}	WHIM descriptor 3rd component accessibility directional
GGI1	-2.943023×10^{-2}	-2.673245×10^{-2}	Topological charge autocorrelations index of order 1
ENEG	2.673222×10^{-2}	-2.428176×10^{-2}	Electronegativity
R7u+	-2.447716×10^{-2}	-2.223341×10^{-2}	GETAWAY descriptor R maximal autocorrelation of lag 7 unweighted
DIPX	-2.397050×10^{-2}	-2.177320×10^{-2}	Dipole moment X
Mor20e	2.249459×10^{-2}	-2.043258×10^{-2}	3D MoRSE descriptor signal 20 weighted by Sanderson electronegativity
Mor11e	-2.069688×10^{-2}	-1.879966×10^{-2}	3D MoRSE descriptor signal 11 weighted by Sanderson electronegativity
PCHGPH	-1.972265×10^{-2}	-1.791474×10^{-2}	Mean partial charge on H atoms
PW2	1.889137×10^{-2}	-1.715966×10^{-2}	Path/walk indices path/walk 2 Randic shape index
RTu+	1.855476×10^{-2}	-1.685390×10^{-2}	GETAWAY descriptor R maximal autocorrelation unweighted

R2u	1.567099×10^{-2}	-1.423448×10^{-2}	GETAWAY descriptor R autocorrelation of lag 2 unweighted
G2v	1.563596×10^{-2}	-1.420266×10^{-2}	WHIM descriptor 2nd component symmetry directional weighted by van der Waals volume
FDI	-1.196298×10^{-2}	-1.086637×10^{-2}	Distance/distance matrix (G/D) leading eigenvalue from distance/distance matrix
R8u+	-9.157233×10^{-3}	-8.317818×10^{-3}	GETAWAY descriptor R autocorrelation of lag 8 unweighted
RDF065m	6.460672×10^{-3}	-5.868443×10^{-3}	Radial Distribution Function 065 weighted by mass
SCOUNT(C-atom)	-2.090814×10^{-3}	-1.899156×10^{-3}	Substructure count
PCHGMHT	9.051149×10^{-4}	-8.221458×10^{-4}	Mean partial charge on heteroatoms